Introducing Nanochemoprevention as a Novel Approach for Cancer Control: Proof of Principle with Green Tea Polyphenol Epigallocatechin-3-Gallate

Imtiaz A. Siddiqui,[1] Vaqar M. Adhami,[1] Dhruba J. Bharali,[2] Bilal B. Hafeez,[1] Mohammad Asim,[1] Sabih I. Khwaja,[1] Nihal Ahmad,[1] Huadong Cui,[2] Shaker A. Mousa,[2] and Hasan Mukhtar[1]

[1]Department of Dermatology, University of Wisconsin, Madison, Wisconsin; and [2]Pharmaceutical Research Institute at Albany, Albany College of Pharmacy, Albany, New York

Abstract

Chemoprevention, especially through the use of naturally occurring phytochemicals capable of impeding the process of one or more steps of carcinogenesis process, is a promising approach for cancer management. Despite promising results in preclinical settings, its applicability to humans has met with limited success largely due to inefficient systemic delivery and bioavailability of promising chemopreventive agents. Here, we introduce the concept of nanochemoprevention, which uses nanotechnology for enhancing the outcome of chemoprevention. We encapsulated green tea polyphenol epigallocatechin-3-gallate (EGCG) in polylactic acid–polyethylene glycol nanoparticles and observed that encapsulated EGCG retains its biological effectiveness with over 10-fold dose advantage for exerting its proapoptotic and angiogenesis inhibitory effects, critically important determinants of chemopreventive effects of EGCG in both *in vitro* and *in vivo* systems. Thus, this study could serve as a basis for the use of nanoparticle-mediated delivery to enhance bioavailability and limit any unwanted toxicity of chemopreventive agents, such as EGCG. [Cancer Res 2009;69(5):1712–6]

Introduction

Cancer remains one of the most devastating diseases in the world amid epidemiologic studies suggesting that cancer will be the number one disease in prevalence by 2020 (1). Chemoprevention via the use of naturally occurring nontoxic agents has emerged as a plausible strategy for cancer management (2). Despite promising results in preclinical settings, the applicability of chemoprevention to human has met with only limited success, largely due to inefficient systemic delivery and bioavailability of promising agents. Therefore, to achieve maximum response of a chemopreventive agent, novel strategies are required to enhance the bioavailability of potentially useful agents and reduce perceived toxicity. We envisioned that nanoparticle-mediated delivery could be useful to limit the toxicity and enhance the bioavailability of the chemopreventive agents. It is noteworthy that, in recent years, nanotechnology is being implemented and assessed in different areas of cancer therapeutics and cancer management (3). However, the use of nanotechnology has not been pursued to improve the outcome of chemopreventive strategies. In this study, we have assessed the effectiveness of delivery of epigallocatechin-3-gallate (EGCG), encapsulated in polylactic acid (PLA)–polyethylene glycol (PEG) nanoparticles against human prostate cancer (PCa) cells under *in vitro* and *in vivo* situations. Our choice for the selection of EGCG and PCa in this study is based on several facts. PCa is one of the most prevalent cancers among men, accounting for an estimated 186,320 new cases and 28,660 deaths in 2008 in the United States alone (4). EGCG is a well-studied chemopreventive agent and has shown remarkable chemopreventive potential in a wide range of cell culture and preclinical studies (5, 6). Furthermore, few best evidences of the cancer chemopreventive effects of EGCG come from PCa (6, 7).

Since most biological processes, including those that are cancer-related, occur at nanoscale, nanoparticulate technology is a potential tool to diagnose and treat cancer. The structure and tunable surface functionality of nanoparticles allow them to encapsulate/conjugate single or multiple entities either in the core or on the surface, rendering them ideal carriers for various anticancer drugs (8). Nanoparticles made up of the biodegradable and biocompatible polymers like PLA, PLGA, starch, etc., have been studied for the delivery of various drugs (8, 9). A significant advantage of these biodegradable polymers is their history of safe use, proven biocompatibility, and ability to control the time and rate of polymer degradation and the release of the incorporated entity. When PLA/PLGA nanoparticles are injected systemically for drug delivery, they are rapidly cleared by the mononuclear phagocytic system by the process of endocytosis, thereby minimizing carrier-induced undesirable cytotoxicity (10). It is well known that the presence of a hydrophilic polymer-like PEG increases the circulation time of nanoparticles by stabilizing them against opsonization (8). PEGylation (i.e., the attachment of PEG to proteins and drugs) is an upcoming methodology for drug development, and it has the potential to revolutionize medicine by drastically improving the pharmacokinetic and pharmacodynamic properties of administered drugs (11).

Materials and Methods

Nanoformulation. PLA-PEG (150–200 μL; 80 mg/mL in DMSO) and EGCG (100 μL; 100 mg/mL DMSO) were mixed together. This mixture of PLA-PEG and EGCG was added drop wise to 20 mL of 2% (w/v) polyvinyl alcohol solution with constant stirring. Resulting solution was sonicated for 10 to 30 s and then stirred using magnetic stirring for 3 h. It was than dialyzed to remove the nonencapsulated EGCG from the solution. Finally, the solution was lyophilized to obtain the nanoformulation in powder form, which was readily soluble in PBS. Characterization of the nanoparticles was done by particle size analysis (Supplementary Fig. S1), transmission electron microscopy (Supplementary Fig. S2), and ζ potential measurement

Note: Supplementary data for this article are available at Cancer Research Online (http://cancerres.aacrjournals.org/).

Requests for reprints: Hasan Mukhtar, Department of Dermatology, University of Wisconsin, Medical Sciences Center, B-25, 1300 University Avenue, Madison, WI 53706. Phone: 608-263-3927; Fax: 608-263-5223; E-mail: hmukhtar@wisc.edu.

doi:10.1158/0008-5472.CAN-08-3978

(Supplementary Fig. S3). The amount of the encapsulated EGCG was determined by forced degradation of the nanoparticles. The concentration of encapsulated EGCG was determined by high-performance liquid chromatography.

Cell viability. Cells were treated with EGCG formulations or PLA-PEG nanoparticles dissolved in PBS. The effect of the treatment on the viability of cells was determined by the 3-(4,5-dimethylthiazol-2-yl)-2,5-diphenyltetrazolium bromide (MTT) assay, as described previously (12).

Protein extraction and Western blotting. Protein extraction and Western blotting was performed, as described previously (12).

Detection of apoptosis. The Annexin V–FLUOS staining assay for apoptosis was performed, as described previously (13). Furthermore, apoptosis was also quantified by terminal deoxynucleotidyl transferase-mediated dUTP-biotin nick and labeling assay, as described previously (14).

Colony formation assay. Cells (8×10^3) were seeded in tissue culture dishes and treated with desired EGCG formulation after 24 h. The cells were maintained under standard cell culture conditions at 37°C and 5% CO_2 in a humid environment. Colonies that formed in 2 to 3 wk were fixed with 10% buffered formalin, stained with 2% gentian violet (w/v methanol solution), washed with water, and air-dried.

Chick chorioallantoic membrane assay. Chick chorioallantoic membrane (CAM) assay was performed, as described previously (15).

***In vivo* tumor xenograft studies.** Tumor xenografts were established, as described previously (13). The mice were then randomly divided into three groups of seven animals each. Group I mice (control) did not receive any treatment; group II mice each received 100 μg of EGCG encapsulated in PLA-PEG nanoparticles (hereafter called 'nano-EGCG') dissolved in PBS thrice weekly; group III mice each received 1 mg of nonencapsulated EGCG dissolved in PBS thrice weekly. Tumor growth was determined in terms of volume of tumors (mm^3) as a function of time. At the termination of the study (when the tumor volume reached 1,300 mm^3 in the control group), tumors were excised, snap frozen in liquid nitrogen, and stored at −80°C. Blood samples were collected either by the "mandibular bleed" or by the "retro-orbital bleed." The serum was separated, by allowing the blood to clot and centrifuging it for 20 min at 4°C, and stored at −80°C for further analysis.

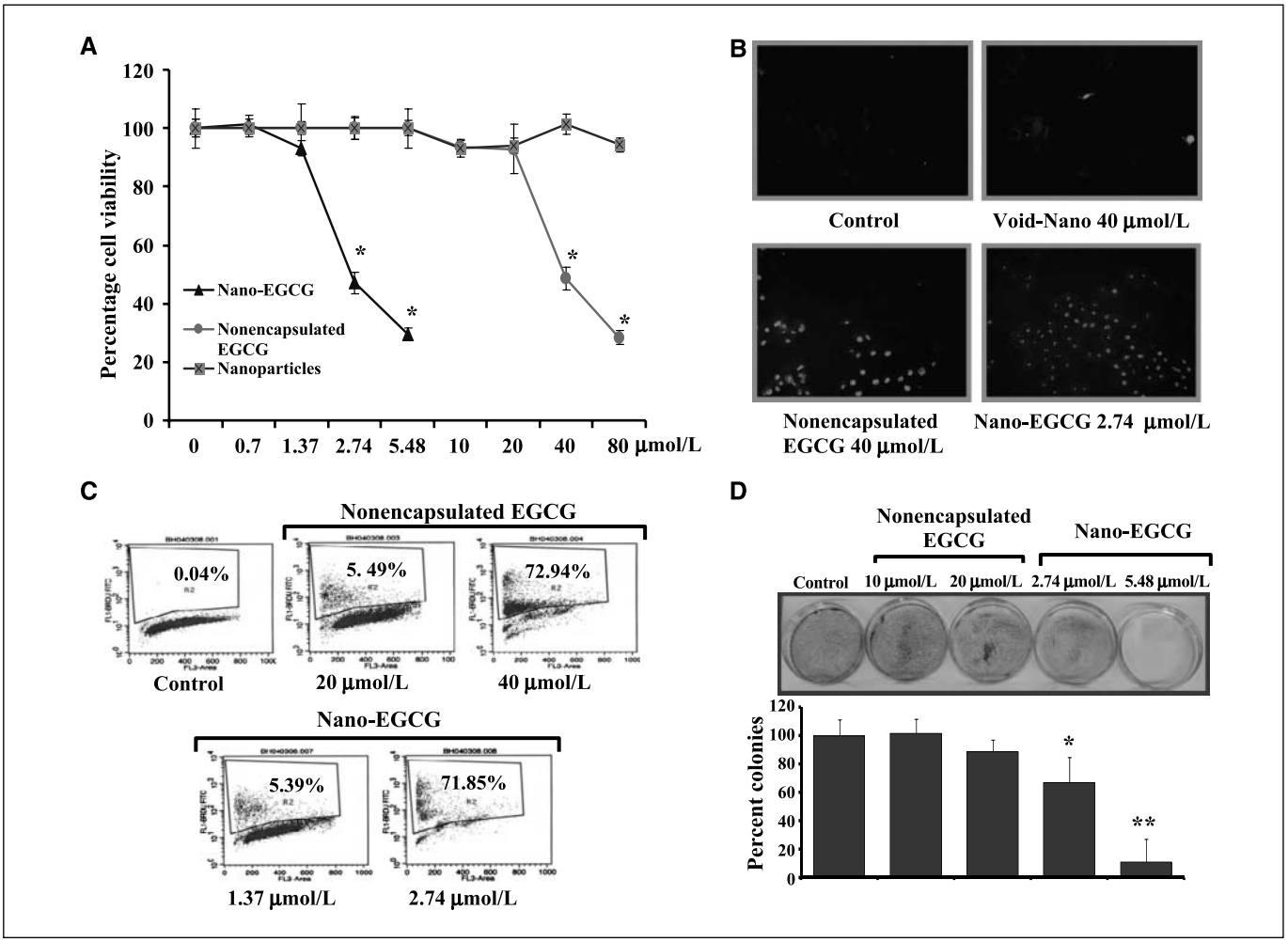

Figure 1. Comparative effects of nonencapsulated EGCG and nano-EGCG treatment on cell viability and apoptosis. *A,* cell growth analysis. PC3 cells were treated with EGCG, void nanoparticles, and nano-EGCG for 24 h, and cell growth was determined by MTT assay. *Points,* mean of three separate experiments wherein each treatment was repeated in 10 wells; *bars,* SE. *, $P < 0.001$ compared with the vehicle-treated controls. *B,* apoptosis detection. PC3 cells were grown on cell culture slides and treated with EGCG and nano-EGCG for 48 h. Apoptosis was determined, as detailed in Materials and Methods. Representative photomicrographs from each treatment group showing induction of apoptosis (*green fluorescence*). Data are from experiment repeated thrice with similar results. *C,* quantitative estimation of apoptosis. Cells were treated for 48 h and labeled with dUTP using an Apo-direct apoptosis kit. The values shown indicate the extent of apoptosis. The images are representative of three independent experiments with similar results. *D,* colony formation. PC3 cells were treated with each agent, and the plates were observed for colonies, counted, and plotted as a bar graph. *Bars,* SE. *, $P < 0.05$; **, $P < 0.01$ compared with the vehicle-treated controls. The results are from a representative experiment repeated thrice with similar results.

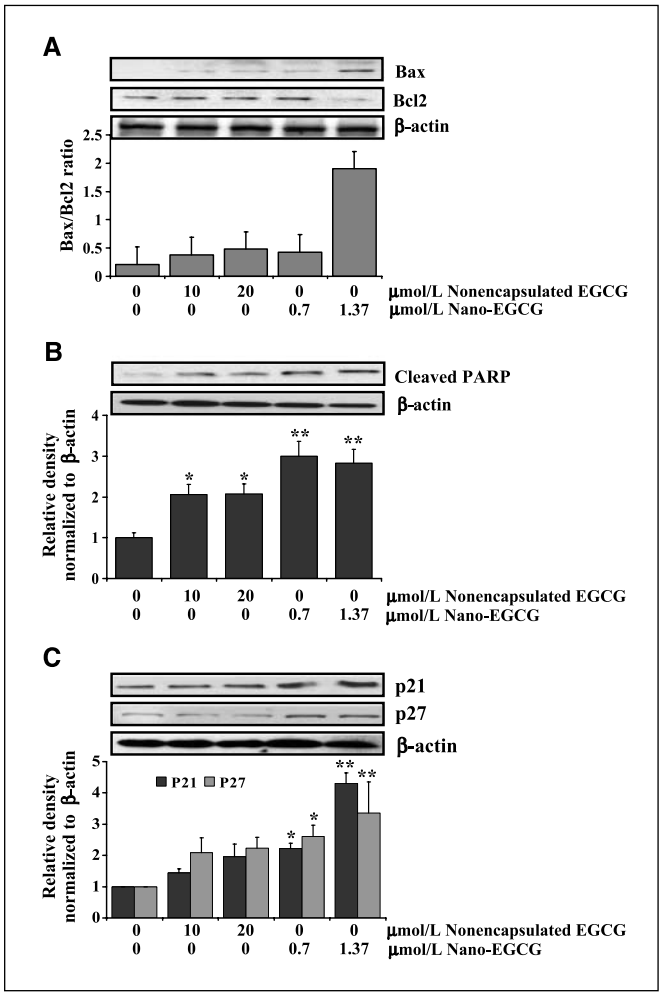

Figure 2. Comparative effects of nonencapsulated EGCG and nano-EGCG on apoptotic biomarkers. *A,* protein expression of Bax, Bcl2, and the Bax/Bcl2 ratio. *B,* protein expression of cleaved PARP. *C,* protein expression of p21 and p27. The cells were treated with each agent and harvested 24 h after treatments. Details of the experiments are described in Materials and Methods. Equal loading was confirmed by stripping the membrane and reprobing it with β-actin. Histograms represent relative densities of the bands normalized to β-actin. *, $P < 0.05$; **, $P < 0.01$ compared with the vehicle-treated controls. Each experiment was repeated thrice with similar results.

To assess the possibility of treatment-toxicity, the effect of treatments on fluid and food consumption and body weight was monitored throughout the study. We did not observe any major difference in weight and fluid intake during the course of study (data not shown).

ELISA for PSA estimation. Commercially available ELISA was performed to quantitate PSA levels in the serum of nude mice, as described previously (13).

LC-MS/MS for analysis of EGCG concentration. Mouse blood was collected immediately, 1, 2, and 4 h after treatment with EGCG formulations. Internal standard (ethyl gallate, 5 μg/mL in 50% methanol) was added to each sample before extraction. For each sample, an aliquot of 80 μL serum was extracted with ethyl acetate and acetonitrile, the supernatant was dried, and the residue was resuspended in 40% acetonitrile. Isocratic chromatography in MRM mode was performed on a SunFire C18 column, kept at 40°C.

Densitometry and statistical analysis. All *in vitro* assays were repeated in three independent experiments, and only representative data are presented. Immunoblots were scanned by HP PrecisionScan Pro 3.13 (Hewlett-Packard). Densitometry measurements of the scanned bands were done using the digitalized scientific software program UN-SCAN-IT (Silk Scientific Corporation). Comparisons between controls and nonencapsulated EGCG–treated or nano-EGCG–treated groups were made using a two-tailed Student's t test, and values of $P < 0.05$ were considered statistically significant.

Results and Discussion

We first compared the effectiveness of nano-EGCG versus nonencapsulated EGCG on proliferative ability in human PCa PC3 cells. Treatment of cells with nanoparticles alone had negligible effect, thereby confirming the lack of any toxicity of nanoparticles (Fig. 1*A*). Interestingly, nano-EGCG, compared with nonencapsulated EGCG, produced remarkably superior effects with over 10-fold dose advantage. As shown in Fig. 1, the IC_{50} value of nano-EGCG (at 24 h posttreatment) was found to be 3.74 μmol/L compared with 43.6 μmol/L of nonencapsulated EGCG. These effects were persistent even at 48 and 72 h posttreatment (Supplementary Fig. S4). Similar effects of nano-EGCG were observed in other PCa cell lines (data not shown), indicating that the effects observed are general and not cell type specific. We observed an efficient uptake of nano-EGCG by PC3 cells (Supplementary Fig. S5), suggesting that nanoencapsulation removes the penetration barriers at cell surfaces. It is possible that nano-EGCG enters into the cells via endocytosis. They adsorb serum proteins nonspecifically onto their surface and enter the cell via receptors on the cell membrane.

We next determined if the effective concentration of EGCG could be lowered by nanoformulation. We observed enhanced apoptosis of PC3 cells treated with nano-EGCG compared with nonencapsulated EGCG. We found that 2.74 μmol/L nano-EGCG cause 72% apoptosis in PC3 cells, whereas, to achieve similar extent of apoptosis, 40 μmol/L of nonencapsulated EGCG were required, thereby providing a remarkable dose advantage (Fig. 1*B* and *C*). Using colony formation assay, nano-EGCG was found to show a remarkable dose advantage (over nonencapsulated EGCG), providing a comparable effect at 5.48 μmol/L nano-EGCG when compared with 40 μmol/L nonencapsulated EGCG (Fig. 1*D*).

Our next goal was to determine if nano-EGCG retains its mechanistic identity. We studied several molecules that have been shown to be affected by EGCG. Our data showed that the key regulators of apoptosis, Bcl-2 family of proteins, were significantly modulated by nano-EGCG. Like nonencapsulated EGCG, nano-EGCG treatment to PC3 cells resulted in a significant increase in proapoptotic Bax with a concomitant decrease in antiapoptotic Bcl-2, thereby shifting the Bax/Bcl-2 ratio in favor of apoptosis (Fig. 2*A*). Furthermore, as shown in Fig. 2*B*, we observed an increase in poly(ADP-ribose) polymerase (PARP) cleavage. Importantly, these responses were observed at a low concentration of nano-EGCG (1.37 μmol/L), further supporting a remarkable dose advantage when EGCG was delivered in nanoparticles. We next assessed the effects of nano-EGCG on induction of the cyclin-dependent kinase inhibitors WAF1/p21 and CIP1/p27. Immunoblot analysis and the densitometric quantitation of protein bands revealed that nano-EGCG resulted in marked induction of p21 and p27 in a dose-dependent manner with a significant dose advantage over EGCG (Fig. 2*C*).

Studies have shown that EGCG is an efficient inhibitor of angiogenesis (16), which has been shown to have a direct correlation with PCa (17). Using CAM assay, we observed a 57% inhibition of fibroblast growth factor (FGF)–induced angiogenesis with nano-EGCG containing only 3 μg EGCG compared with only

35% inhibition with 30 μg nonencapsulated EGCG (Fig. 3*A* and *B*). Furthermore, we observed a significant inhibition of mean branch formation and tumor weight of neuroblastoma-induced angiogenesis in CAM by nano-EGCG (Fig. 3*C* and *D*). These data clearly indicate that although EGCG suppressed angiogenesis in CAM, the concentration required to achieve this inhibition was significantly reduced by its nanoformulation.

To determine the *in vivo* relevance of our *in vitro* findings, we used a xenograft model. We injected athymic nude mice with androgen-responsive 22R*v*1 cells. The choice of 22R*v*1 cells was based on the fact that these cells form rapid tumors with reproducible results and secrete PSA. We compared the effect of nano-EGCG (100 μg/mouse, i.p.) and nonencapsulated EGCG (1 mg/mouse, i.p.) on the growth of tumors. Our data showed that, at 45 days postinoculation, the tumor volume in control mice was 1,242 mm^3 whereas, in both treatment groups, a significant decrease in the tumor volume was observed (nonencapsulated EGCG, 854 mm^3; nano-EGCG, 707 mm^3; $P < 0.01$). These data confirm that, to achieve similar extent of tumor growth inhibition, 10-fold lower dose of nano-EGCG was required (Fig. 4*A* and *B*). We also observed a significant inhibition in serum PSA. The average PSA level in nonencapsulated EGCG–treated mice was found to be significantly decreased to 9.31 (±2.42) ng/mL compared with 29.86 (±8.33) ng/mL in control mice (Fig. 4*C*), whereas the nano-EGCG treatment led to an additional decrease in the levels of serum PSA of 2.64 (± 0.42) ng/mL (Fig. 4*C*). The observed decrease of serum PSA by nano-EGCG at such a low concentration is an important observation, because serum PSA is arguably regarded as the best marker in the diagnosis and prognosis of PCa in human (18).

Limited bioavailability is the major drawback associated with the failure of many naturally occurring chemopreventive agents in clinical settings. As shown by the data in Fig. 4*D*, the rate of degradation of nonencapsulated EGCG was rapid with a complete degradation within 4 h, whereas nano-EGCG had a significantly longer half-life (Fig. 4*D*). Thus, it seems that nanoformulation can enhance the stability of EGCG *in vivo*, providing a target-specific enhanced bioavailability leading to a significantly better clinical outcome. Since EGCG has been shown to act in synergy with other therapeutic approaches (12, 13), we presume that nanoformulation of EGCG will also result in similar effects. Because of enhanced stability, nano-EGCG will provide a much better response when used in combination with other approaches.

In this study, we show the efficacy of nanoparticulate technology to enhance the therapeutic effectiveness of EGCG. Our data clearly suggest that nano-EGCG exhibits >10-fold dose advantage over nonencapsulated EGCG. We also show that EGCG retains its mechanistic signature upon nanoformulation. As with many other nanoparticles, the advantage of using PLA-PEG nanoparticles lies in their high surface area to volume ratio, which presumably allows them to upload more EGCG while maintaining the small size. This is particularly important because the enhanced conjugation of nanoparticles with agents often results in the generation of

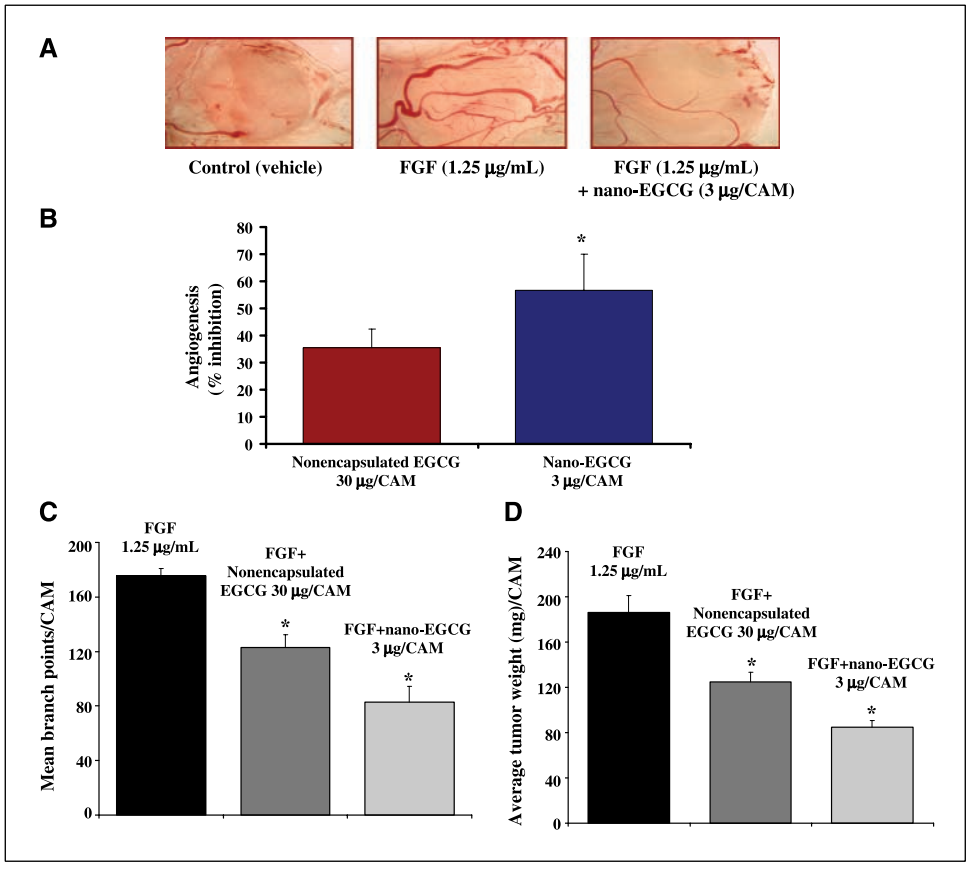

Figure 3. Comparative effects of nano-EGCG and nonencapsulated EGCG on FGF-induced angiogenesis. *A,* CAM assay. Photopictographs of a typical experiment showing the angiogenesis pattern in different treatments. Data are from a typical experiment repeated in five CAM with similar results. *B,* bar graph showing percentage inhibition of angiogenesis in nonencapsulated EGCG–treated and nano-EGCG–treated CAM. *Columns,* data of angiogenesis from experiment done with five CAM membranes with similar results; *bars,* SE. *, $P < 0.05$ compared with the EGCG-treated group. *C,* mean branch points. Mean branch points were counted per CAM. *Columns,* data for inhibition of mean branch points in CAM membranes from a typical experiment repeated in five CAM with similar results; *bars,* ±SE. *, $P < 0.05$ compared with the vehicle-treated controls. *D,* average tumor weight. CAM tumors were excised and weighed 5 d after cell grafting. Data are from a typical experiment repeated in five CAM with comparative results. *, $P < 0.05$ compared with the vehicle-treated controls.

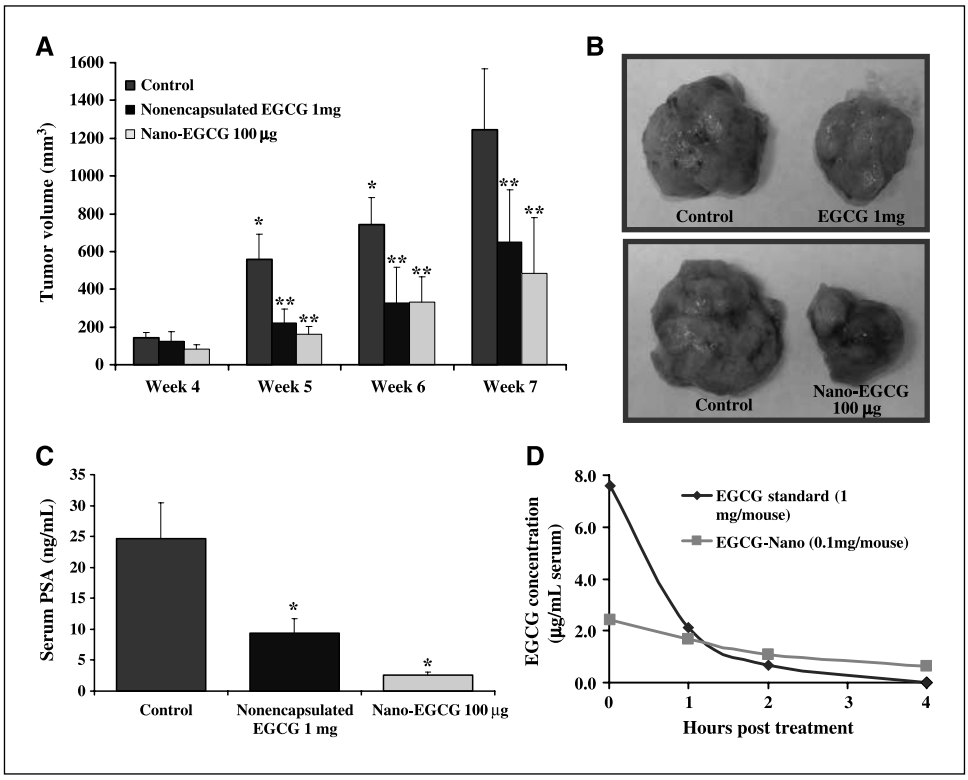

Figure 4. Comparative effects of nonencapsulated EGCG and nano-EGCG on tumor growth and PSA secretion in a xenograft model. *A,* effect on the growth of tumor xenografts. Details of the experiments are given in Materials and Methods. *Columns,* tumor volume (mm^3) of seven mice; *bars,* SE. *, $P < 0.05$ compared with the data from control group at previous time point. **, $P < 0.01$ compared with the control group at the respective time point. *B,* photographs of tumors. Photographs were taken of the excised tumors at the termination of the experiment. Typical tumors from control and treated groups. *C,* effect on the serum PSA levels. The levels of PSA were determined by ELISA assay and expressed as serum (in ng/mL) ± SE of five mice. *, $P < 0.05$ compared with the vehicle-treated controls. *D,* EGCG serum levels. Four mice in each group were treated with the agents and bled immediately and 1, 2, and 4 h after treatment. Serum was separated, and EGCG concentration was determined. Results are expressed as EGCG concentration (μg/mL serum).

nanoparticles that are sparingly taken up by the diseased cells, owing to their bigger size and, thereby, undermining their medical usefulness (19). Also, the therapeutic/clinical importance of PLA-PEG nanoparticles relies on the fact that, being biodegradable, they rarely pose any toxicity (8, 20).

Based on our promising data, we suggest that the concept of nanochemoprevention (i.e., encapsulation of chemopreventive agents in nanoparticles) possesses strong merit and rationale for conducting additional detailed *in vivo* studies in appropriate animal models with relevance to human disease.

Disclosure of Potential Conflicts of Interest

No potential conflicts of interest were disclosed.

Acknowledgments

Received 10/16/2008; revised 12/11/2008; accepted 1/9/2008; published OnlineFirst 02/17/2009.

Grant support: US PHS grants RO1 CA 78809, RO1 CA 101039, and RO1 CA 120451.

The costs of publication of this article were defrayed in part by the payment of page charges. This article must therefore be hereby marked *advertisement* in accordance with 18 U.S.C. Section 1734 solely to indicate this fact.

We thank Lea C. Moody and Saad A. Jaaka for their technical assistance.

References

1. Murray, CJL, Lopez, AD, eds. The global burden of disease: a comprehensive assessment of mortality and disability from diseases, injuries and risk factors in 1990 and projected to 2020. Cambridge, MA: Harvard University Press on behalf of the World Health Organization and the World Bank; 1996.
2. Siddiqui IA, Afaq F, Adhami VM, Mukhtar H. Prevention of prostate cancer through custom tailoring of chemopreventive regimen. Chem Biol Interact 2008;171:122–32.
3. Nishiyama N. Nanomedicine: nanocarriers shape up for long life. Nat Nanotechnol 2007;2:203–4.
4. Jemal A, Siegel R, Ward E, et al. Cancer statistics, 2008. CA Cancer J Clin 2008;58:71–96.
5. Khan N, Afaq F, Saleem M, Ahmad N, Mukhtar H. Targeting multiple signaling pathways by green tea polyphenol (-)-epigallocatechin-3-gallate. Cancer Res 2006;66:2500–5.
6. Stuart EC, Scandlyn MJ, Rosengren RJ. Role of epigallocatechin gallate (EGCG) in the treatment of breast and prostate cancer. Life Sci 2006;79:2329–36.
7. Saleem M, Adhami VM, Siddiqui IA, Mukhtar H. Tea beverage in chemoprevention of prostate cancer: a mini-review. Nutr Cancer 2003;47:13–23.
8. Gref R, Minamitake Y, Peracchia MT, Trubetskoy V, Torchilin V, Langer R. Biodegradable long-circulating polymeric nanospheres. Science 1994;263:1600–3.
9. Peer D, Karp JM, Hong S, Farokhzad OC, Margalit R, Langer R. Nanocarriers as an emerging platform for cancer therapy. Nat Nanotechnol 2007;2:751–60.
10. Nie S, Xing Y, Kim GJ, Simons JW. Nanotechnology applications in cancer. Annu Rev Biomed Eng 2007;9:257–88.
11. Gref R, Domb A, Quellec P, et al. The controlled intravenous delivery of drugs using PEG-coated sterically stabilized nanospheres. Adv Drug Deliv Rev 1995;16:215–33.
12. Siddiqui IA, Malik A, Adhami VM, et al. Green tea polyphenol EGCG sensitizes human prostate carcinoma LNCaP cells to TRAIL-mediated apoptosis and synergistically inhibits biomarkers associated with angiogenesis and metastasis. Oncogene 2008;27:2055–63.
13. Adhami VM, Malik A, Zaman N, et al. Combined inhibitory effects of green tea polyphenols and selective cyclooxygenase-2 inhibitors on the growth of human prostate cancer cells both *in vitro* and *in vivo*. Clin Cancer Res 2007;13:1611–9.
14. Saleem M, Maddodi N, Abu Zaid M, et al. Lupeol inhibits growth of highly aggressive human metastatic melanoma cells *in vitro* and *in vivo* by inducing apoptosis. Clin Cancer Res 2008;14:2119–27.
15. Mousa SA, O'Connor LJ, Bergh JJ, Davis FB, Scanlan TS, Davis PJ. The proangiogenic action of thyroid hormone analogue GC-1 is initiated at an integrin. J Cardiovasc Pharmacol 2005;46:356–60.
16. Cao Y, Cao R. Angiogenesis inhibited by drinking tea. Nature 1999;398:381.
17. Daliani D. Development of angiogenesis inhibition as therapy for prostate cancer. Oncology (Huntingt) 2000;14:21–3.
18. Pound CR, Partin AW, Eisenberger MA, Chan DW, Pearson JD, Walsh PC. Natural history of progression after PSA elevation following radical prostatectomy. JAMA 1999;281:1591–7.
19. Balogh L, Nigavekar SS, Nair BM, et al. Significant effect of size on the *in vivo* biodistribution of gold composite nanodevices in mouse tumor models. Nanomedicine 2007;3:281–96.
20. Zhang L, Gu FX, Chan JM, Wang AZ, Langer RS, Farokhzad OC. Nanoparticles in medicine: therapeutic applications and developments. Clin Pharmacol Ther 2008;83:761–9.